

RESOLVED SPECTROSCOPY OF M DWARF/L DWARF BINARIES. III. THE “WIDE” L3.5/L4 DWARF BINARY 2MASS J15500845+1455180AB

ADAM J. BURGASSER^{1,2}

Center of Astrophysics and Space Sciences, Department of Physics, University of California, San Diego, CA 92093, USA;
aburgasser@ucsd.edu

SAURAV DHITAL

Department of Physics & Astronomy, Vanderbilt University, Nashville, TN 37235, USA

AND

ANDREW A. WEST¹

Institute for Astrophysical Research, Boston University, Boston, MA 02215, USA

Submitted to AJ on 4 August 2009; accepted for publication 16 September 2009

ABSTRACT

We report the identification of 2MASS J15500845+1455180 as a 0^o.9 L dwarf visual binary. This source is resolved in Sloan Digital Sky Survey (SDSS) images and in near-infrared imaging with the IRTF SpeX imager/spectrometer. The two components, oriented along a north-south axis, have similar brightnesses in the near-infrared ($\Delta K \approx 0.2$ mag), although the fainter northern component is redder in $J - K$ color. Resolved near-infrared spectroscopy indicates spectral types of L3.5 and L4, consistent with its L3 combined-light optical classification based on SDSS data. Physical association is confirmed through common proper motion, common spectrophotometric distances and low probability of chance alignment. The projected physical separation of 2MASS J1550+1455AB, 30 ± 3 AU at an estimated distance of 33 ± 3 pc, makes it the widest L dwarf-L dwarf pair identified to date, although such a separation is not unusual among very low-mass field binaries. The angular separation and spectral composition of this system makes it an excellent target for obtaining a precise lithium depletion age, and a potential age standard for low-temperature atmosphere studies.

Subject headings: binaries: visual — stars: individual (2MASS J15500845+1455180) — stars: low mass, brown dwarfs

1. INTRODUCTION

Very low-mass (VLM) stars and brown dwarfs—with masses less than $0.1 M_{\odot}$ —are among the most populous but least understood stellar populations in the Galaxy. Encompassing the low-mass tail of the stellar/substellar mass function, these faint and low effective temperature (T_{eff}) sources are incompletely sampled even in the immediate vicinity of the Sun (e.g., Reid et al. 1995; Henry et al. 2006). Over the past decade, wide-field red optical and near-infrared sky surveys have facilitated the discovery of thousands of new nearby VLM sources, including members of the recently defined L and T spectral classes (Kirkpatrick 2005). These include roughly 100 VLM multiple systems,³ estimated to comprise 20–25% of the population (Basri & Reiners 2006; Allen 2007).

Studies of VLM multiples have focused in large part on the very tightest (angular separations $\rho \lesssim 0\prime.1$, projected physical separations $a \lesssim 0.1$ –1 AU) and the very widest pairs ($\rho \gtrsim 1\prime$, $a \gtrsim 10$ –100 AU). The short pe-

riods of the former are useful for Keplerian mass measurements and radius measurements (e.g., Stassun et al. 2006), both required to test low-mass stellar structure models (e.g., Chabrier et al. 2009). For those systems with independent age determinations (cluster members, companions to age-dated stars), these measurements also serve to test evolutionary theory (Zapatero Osorio et al. 2004; Dupuy et al. 2009). The identification and study of tight VLM multiples is challenged, however, by the need for adaptive optics-enhanced and/or space-based high-resolution imaging, and in a few cases large-aperture high resolution spectroscopic monitoring (Reid et al. 2002; Basri & Reiners 2006; Joergens & Müller 2007).

In contrast, wide VLM multiples have prohibitively long orbits for mass measurements, but detailed investigations of their coeval components can be made. These systems facilitate comparative analyses of low-temperature atmospheres and magnetic emission in the absence of age and composition dependencies (e.g., Burgasser & McElwain 2006; McElwain & Burgasser 2006; Martín et al. 2006; Kasper et al. 2009). Wide VLM pairs are also relatively rare, with systems wider than $a \gtrsim 20$ AU comprising $\lesssim 2\%$ of all VLM multiples in the field (Allen 2007; Caballero 2007a), although a few systems exceeding 1000 AU separation have been identified (e.g., Caballero 2007b; Artigau et al. 2007; Radigan et al. 2009). The rarity of wide VLM binaries in the field and in some young clusters (e.g., Kraus & Hillenbrand 2009) may be a conse-

¹ Also Massachusetts Institute of Technology, Kavli Institute for Astrophysics and Space Research, 77 Massachusetts Avenue, Cambridge, MA 02139, USA

² Visiting Astronomer at the Infrared Telescope Facility, which is operated by the University of Hawaii under Cooperative Agreement no. NCC 5-538 with the National Aeronautics and Space Administration, Science Mission Directorate, Planetary Astronomy Program.

³ A current list is maintained at the VLM Binaries Archive, <http://www.vlmbinaries.org>.

quence of formation mechanisms unique to VLM stars and brown dwarfs (e.g., embryonic dynamical ejection: Reipurth & Clarke 2001; Bate et al. 2002; fragmentation of circumstellar disks: Boss 2001; Jiang et al. 2004) or dynamical evolution within and/or outside the natal cloud (e.g., Close et al. 2007). In addition, wide VLM pairs are often found to be triples or quadruples (e.g., Phan-Bao et al. 2006; S. Dhital et al. 2009, in preparation), enabling studies of higher order multiplicity associated with star and brown dwarf formation.

In this article, we report the discovery of a new wide L dwarf pair, 2MASS J15500845+1455180 (hereafter 2MASS J1550+1455; Cruz et al. 2007) identified by direct imaging and resolved spectroscopy to be a $0''.9$, near-equal brightness binary. In Section 2 we describe imaging and spectroscopic observations of the source, and ascertain the separation, relative near-infrared magnitudes and individual spectral classifications of its components. In Section 3 we review evidence that this source is a physical binary based on constraints in common proper motion, common spectrophotometric distances and low probability of chance alignment. The properties of 2MASS J1550+1455 are discussed in the context of other VLM binaries in Section 4, along with motivation to measure its age using the binary brown dwarf Li I test. Results are summarized in Section 5.

2. OBSERVATIONS

2.1. Target Properties and SDSS Measurements

2MASS J1550+1455 was originally identified by Cruz et al. (2007) in a color- and magnitude-selected search of the Two Micron All Sky Survey (2MASS; Skrutskie et al. 2006) for nearby late-type M and L dwarfs. It was selected as a near-infrared bright ($K_s = 13.26 \pm 0.04$ mag) but optically faint source with red near-infrared colors ($J - K_s = 1.52 \pm 0.05$ mag). The epoch 2009 February 6 (UT) 2MASS images show an unresolved point source. Cruz et al. (2007) reported an optical spectral classification of L2: on the Kirkpatrick et al. (1999) scale, the uncertainty arising from low signal-to-noise data (I. N. Reid & K. L. Cruz, 2009, private communication). 2MASS J1550+1455 has a relatively small proper motion, $\mu = 0.165 \pm 0.015'' \text{ yr}^{-1}$ (Jameson et al. 2008), which combined with the 31 pc distance estimate of Cruz et al. (2007) yields an estimated tangential velocity $V_{\text{tan}} = 24 \text{ km s}^{-1}$, typical for a “normal” thin disk L dwarf (e.g., Faherty et al. 2009).

2MASS J1550+1455 was also imaged and targeted for spectroscopy by the Sloan Digital Sky Survey (SDSS; York et al. 2000). This source is morphologically classified in SDSS as a galaxy due to its extended point spread function (PSF), as shown in Figure 1. Both i - and z -band images show a faint extension toward the north, which as discussed below is consistent with a faint, marginally resolved companion. Spectroscopic data from SDSS Data Release 7 (DR7; Abazajian et al. 2009) are shown in Figure 2. These data are superior to those in the Cruz et al. (2007) study, and comparison to the Kirkpatrick et al. (1999) spectral standards indicate an optical classification of L3 (an uncertainty of 0.5 subtypes is assumed). There is no indication of either H α emission (6563 Å) or Li I absorption (6708 Å) to limiting pseudo-equivalent

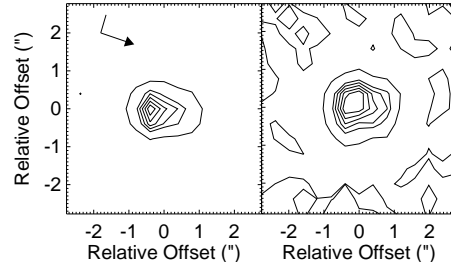


FIG. 1.— Contour plots of flux in epoch 2005 March 10 (UT) SDSS i - (left) and z -band images (right) at the position of 2MASS J1550+1455. Contours of 0.98, 0.96, 0.94, 0.92, 0.9, 0.85 and 0.8 times the peak flux of the central source are shown. The axis scale is arcseconds on the sky relative to the SDSS coordinates. The orientation of the images is indicated by the arrow (head to north, foot to east).

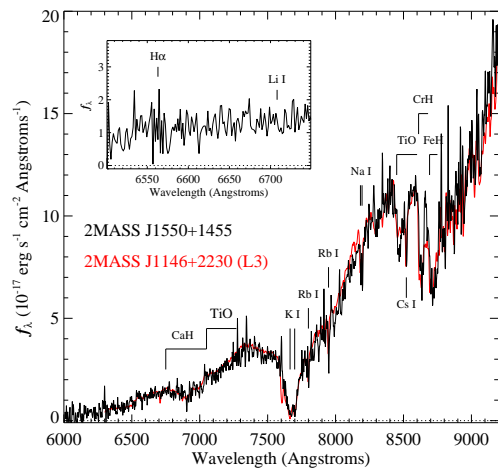


FIG. 2.— SDSS spectrum of 2MASS J1550+1455 (thin black line) compared to the L3 spectral standard 2MASS J1146345+223053 (thick red line; Kirkpatrick et al. 1999). Both spectra are smoothed to a common resolution of $\lambda/\Delta\lambda = 1500$, and the standard spectrum is scaled to match the SDSS spectrum at 8400 Å. Key spectral features are labeled. Inset box shows the region around H α (6563 Å) and Li I lines (6708 Å) in the unsmoothed SDSS spectrum of 2MASS J1550+1455.

widths⁴ of -1.8 \AA and 1.2 \AA , respectively. We infer a radial velocity for 2MASS J1550+1455 of $-7 \pm 12 \text{ km s}^{-1}$ based on cross-correlation with similarly-typed L dwarf velocity templates also observed by SDSS (S. Schmidt et al., in preparation).

2.2. Imaging Observations

2MASS J1550+1455 was targeted with the 3 m NASA Infrared Telescope Facility (IRTF) SpeX spectrograph (Rayner et al. 2003) on 2009 June 29 (UT), as part of a program to identify unresolved L dwarf/T dwarf spectral binaries (e.g., Burgasser et al. 2008a). Conditions were clear with excellent seeing of $0''.4$ – $0''.5$ at J - and K -bands. Acquisition images obtained with SpeX’s imaging channel revealed two point sources at the position of 2MASS J1550+1455 aligned along a north-south axis, in the same orientation as the SDSS extended PSF. Four 20 s dithered exposures were obtained at an airmass of

⁴ Equivalent widths relative to the local continuum.

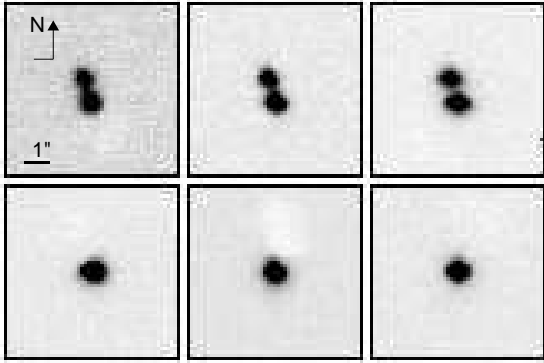


FIG. 3.— SpeX images of 2MASS J1550+1455AB (top) and the nearby point source 2MASS J15504059+1500305 (bottom) in the J -, H - and K -bands (left to right). The images show $6''.12 \times 6''.12$ (51×51 pixels) regions around both sources, aligned with north up and east to the left.

1.31 in each of the MKO⁵ J , H , and K filters. We also obtained two 20 s dithered images of the nearby ($\rho \sim 9.4'$) point source 2MASS J15504059+1500305 ($K_s = 13.11 \pm 0.03$ mag, $J - K_s = 0.73 \pm 0.04$ mag) in each of the JHK filters immediately after the 2MASS J1550+1455 observation to serve as a PSF calibrator.

Imaging data were reduced in a standard manner using custom Interactive Data Language (IDL) routines. After mirror-flipping the raw imaging data along the y -axis to reproduce the sky orientation (J. T. Rayner, 2009, private communication), sky images for each filter were produced by median-combining all of the 2MASS J1550+1455 and PSF calibrator images. These were subtracted from the raw imaging data, and each sky image was also normalized and used as a flat-field frame to correct for pixel-to-pixel response variations. Subsections of each image, 51 pixels ($6''.12$) on a side and centered on the target source, were extracted from these calibrated frames. A final image for each filter/target pair was produced by averaging the registered subframes together, rejecting 5σ pixel outliers for the 2MASS J1550+1455 observations. These combined images are shown in Figure 3. The two components of 2MASS J1550+1455 are clearly resolved, separated by roughly $1''$ along a nearly north-south axis, the southern component appearing to be slightly brighter in all three filter bands. Hereafter, we refer to this component as 2MASS J1550+1455A and the northern component as 2MASS J1550+1455B.

2.3. PSF Fitting

Component magnitudes and the angular separation of the 2MASS J1550+1455 pair were determined by PSF fits to the reduced imaging data, following the prescription described in McElwain & Burgasser (2006). Fits were made to each individual image frame using both PSF calibrator images in a given filter band, for a total of eight independent measures of the relative JHK component magnitudes and 24 independent measures of the separation and orientation of the pair. Measurements of the latter were converted from pixels to arcseconds assuming a plate scale of $0''.120 \pm 0''.002$ pixel⁻¹ (J. T. Rayner, 2005, private communication) and no distortion.

⁵ Mauna Kea Observatory filter system; see Tokunaga et al. (2002) and Simons & Tokunaga (2002).

TABLE 1
RESULTS OF PSF FITTING

Parameter	Value
SDSS Epoch 2005 March 10 (UT)	
$\Delta \alpha \cos \delta$ ($''$) ^a	0.24 ± 0.04
$\Delta \delta$ ($''$) ^a	0.92 ± 0.06
ρ ($''$)	0.95 ± 0.06
θ ($^\circ$) ^a	14.5 ± 1.3
Δi (mag)	0.8 ± 0.3
Δz (mag)	0.7 ± 0.3
SpeX Epoch 2009 June 29 (UT)	
$\Delta \alpha \cos \delta$ ($''$) ^a	0.26 ± 0.02
$\Delta \delta$ ($''$) ^a	0.87 ± 0.03
ρ ($''$)	0.91 ± 0.03
θ ($^\circ$) ^a	16.6 ± 1.3
ΔJ (mag)	0.41 ± 0.03
ΔH (mag)	0.29 ± 0.05
ΔK (mag)	0.23 ± 0.03

^a Angular separation (ρ) and position angle (θ) measured from the brighter primary to the fainter secondary.

The position angle was assumed to be accurate to within $0^\circ.25$ (ibid.).

To test for systematic effects in the derived relative magnitudes, we performed the same fits on synthetic binary images constructed from the PSF frames. For each filter, synthetic images were made by combining two randomly selected calibrator images, one shifted according to the measured separations (with an additional random shift based on the separation uncertainties) and scaled by flux ratios spanning 0.2 to 1.0 (magnitude differences of 1.75 to 0 mag). A linear fit between input and output flux ratios for 200 trials indicates systematic shifts of 3–7% depending on the filter band (largest at K), which were incorporated into the reported photometry and uncertainties.

Results are listed in Table 1. The angular separation of the pair is inferred to be $0''.91 \pm 0''.03$ at a position angle of $16^\circ.6 \pm 1^\circ.1$ (east of north, vector pointing from primary to secondary). The magnitude differences of the two components decrease from J to K , indicating a secondary that is significantly redder than the primary, $J - K_s = 1.63 \pm 0.06$ mag versus 1.43 ± 0.06 mag.⁶ As described below, this is consistent with the slightly later spectral classification inferred for this component.

We performed the same analysis on the epoch 2005 March 10 (UT) SDSS i and z images, using three nearby point sources as PSF calibrators. The coarser plate scale of the SDSS images ($0''.396$ pixel⁻¹; Pier et al. 2003) and larger PSFs result in both larger astrometric uncertainties and larger systematic offsets in the relative photometry (up to 30%, based on simulations equivalent to those described above). Nevertheless, the inferred separation and orientation of the components formally agree with the SpeX results. There is also an indication that the northern component is considerably fainter in the SDSS bands, $\Delta i = 0.8 \pm 0.3$ mag and $\Delta z = 0.7 \pm 0.3$ mag.

2.4. Spectroscopic Observations

⁶ These colors are on the 2MASS photometric system, based on the MKO to 2MASS photometric conversions described in Section 3.

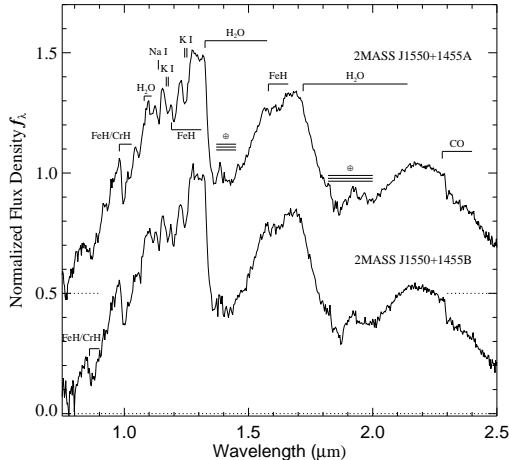


FIG. 4.— Near-infrared spectra of 2MASS J1550+1455A (top) and 2MASS J1550+1455B (bottom) obtained with IRTF/SpeX. Data are normalized at the 1.3 μm spectral peak, with the spectrum of 2MASS J1550+1455A offset by a constant for clarity (dotted lines). Near-infrared spectral features characteristic of L dwarfs are labeled.

Both components of 2MASS J1550+1455 were also observed on 2009 June 29 (UT) with the prism-dispersed mode of SpeX, which provides 0.75–2.5 μm continuous spectroscopy with resolution $\lambda/\Delta\lambda \approx 120$ for the 0".5 slit employed (dispersion across the chip is 20–30 \AA pixel⁻¹). The components were observed simultaneously by aligning the slit to a position angle of 15°; note that this is 62° off from the parallactic angle, so some wavelength-dependent light loss is expected (although it was somewhat mitigated by the excellent seeing; see Burgasser et al. 2007). Six exposures of 120 s each were obtained over an airmass ranging from 1.25 to 1.29, dithering in an ABBA pattern along the slit. Guiding was performed on spillover light from the brighter component, imaged through the H+K notch filter on the SpeX imaging channel. For telluric absorption correction and flux calibration, we observed the nearby ($\rho = 7''.1$) A0 V star HD 136831 within an hour of the 2MASS J1550+1455 observation, at a similar airmass (1.20) and using the same instrument configuration, but with the slit aligned along the parallactic angle. Data were reduced using the SpeXtool package, version 3.3 (Vacca et al. 2003; Cushing et al. 2004) with standard settings; see Burgasser et al. (2007) for details. We took care in the extraction step to select only the opposite wings of the spatial PSF profiles of each component in order to minimize flux contamination. Based on the width of these profiles (full width at half maximum of $\sim 0''.5$), the separation of the components ($0''.9$; see below) and their similar brightnesses, we estimate no more than 5–10% contamination in either spectrum over the 1.0–2.4 μm range.

The reduced spectra for both components are shown in Figure 4. Both exhibit classic signatures of L dwarf near-infrared spectra: deep H₂O absorption bands centered at 1.4 and 1.9 μm ; strong CO absorption at 2.3 μm ; strong FeH absorption at 0.86, 0.99 and 1.6 μm ; unresolved K I and Na I doublets at 1.14, 1.17 and 1.25 μm ; no detectable Na I absorption at 2.2 μm (absent in L2 and later dwarfs; McLean et al. 2003); and a steep 0.8–

TABLE 2
NEAR INFRARED SPECTRAL INDICES

Index	2MASS J1550+1455A		2MASS J1550+1455B		Reference
	Value	SpT	Value	SpT	
H ₂ O-J	0.827	L3.5	0.786	L4.5	1,2
H ₂ O-H	0.776	L3.5	0.739	L5	1,2
CH ₄ -K	1.064	L2 ^a	1.040	L4	1,2
H ₂ O-A	0.634	L3	0.607	L4	3
H ₂ O-B	0.691	L3.5	0.663	L4	3
K I	0.268	L3	0.297	L3.5	3,4
H ₂ O-1.5 μm	1.437	L3	1.526	L4	5
CH ₄ -2.2 μm	0.940	L3/L4	0.962	L4	5

REFERENCES. — (1) Burgasser et al. (2006); (2) Burgasser (2007); (3) Reid et al. (2001); (4) Tokunaga & Kobayashi (1999); (5) Geballe et al. (2002).

^a Not used to compute final (mean) classification of this source.

1.2 μm spectral slope. Both spectra appear to be representative of normal L dwarfs, lacking the extremely red or extremely blue spectral energy distributions found in young/dusty and old/metal-poor L dwarfs, respectively (e.g., Burgasser et al. 2003a; Allers et al. 2007;Looper et al. 2008b). H₂O and FeH absorption is somewhat deeper in the fainter component; note in particular the depths of the 1.3 μm and 0.86 μm bands, respectively.

Near-infrared classifications for each spectrum were derived using a suite of spectral indices and spectral type/index relations defined by Tokunaga & Kobayashi (1999); Reid et al. (2001); Geballe et al. (2002); Burgasser et al. (2006); and Burgasser (2007). Table 2 lists the values of eight indices sampling the prominent H₂O bands and shape of the K-band peak. The subtypes inferred from these indices are nearly all in agreement, with the exception of the CH₄-K index for 2MASS J1550+1455A which is not particularly sensitive to early-L subtype. Ignoring this index, we infer average types of L3.5 and L4 for 2MASS J1550+1455A and 2MASS J1550+1455B, respectively, with scatter of 0.3–0.4 subtypes. These classifications are formally consistent with the L3 combined-light optical classification of the system, particularly as the secondary is considerably fainter than the primary at these wavelengths. Note that each index consistently classifies the B component 0.5–1.5 subtypes later than the A component.

The near-infrared types of 2MASS J1550+1455A and 2MASS J1550+1455B correspond to effective temperatures $T_{\text{eff}} \approx 1910 \pm 110$ K and 1840 ± 110 K, respectively, according to the T_{eff} /spectral type relation ofLooper et al. (2008a, uncertainties include classification error and scatter in relation). Estimates of the component masses for ages of 0.5, 1 and 5 Gyr based on these temperatures and the evolutionary models ofBurrows et al. (1997) are listed in Table 3; estimate are roughly 10% smaller for the DUSTY and COND evolutionary models of Chabrier & Baraffe (2000) and Baraffe et al. (2003). Note that the near-unity mass ratio of this system, $q \equiv M_2/M_1 > 0.95$ for ages of 0.5–5 Gyr, is typical of the majority of VLM binaries (Allen 2007).

3. IS 2MASS J1550+1455 A PHYSICAL BINARY?

The presence of two similarly-typed, near equal-brightness L dwarfs at the position of

2MASS J1550+1455 strongly suggests a physically bound pair, and we examined three lines of evidence for association: common proper motion, common distance, and low probability of chance alignment or random pairing. For the first criterion, the detection of the secondary in both SDSS and SpeX images provides a stringent constraint on the relative motion of the two sources over the intervening 4.3 yr. Assuming that the component alignment is the same in both epochs (i.e., that the northern component is the same star in both images), we infer relative motions of 4 ± 10 mas yr⁻¹ in Right Ascension and -12 ± 15 mas yr⁻¹ in declination; i.e., consistent with no relative motion. These limits correspond to a relative tangential velocity of $V_{\text{tan}} \leq 3$ km s⁻¹ at the adopted distance of 2MASS J1550+1455 (see below), of order their estimated orbital velocities (~ 1 km s⁻¹; see below). We therefore rule out significant differential motion between the components of this system.

For the second criterion, distances were computed from the individual component near-infrared magnitudes, using the combined light 2MASS photometry and relative photometry from our SpeX measurements; see Table 3.⁷ These magnitudes, combined with the M_J /spectral type relation of Cruz et al. (2003), indicate spectrophotometric distance estimates of 31 ± 3 pc for the primary and 34 ± 3 pc for the secondary, where the uncertainties include both photometric uncertainties and scatter in the Cruz et al. relation. These distances agree to within the uncertainties and are consistent with an average distance of 33 ± 3 pc.

Finally, we calculated the probability of chance alignment based on the three dimensional position of 2MASS J1550+1455 in the Galaxy. S. Dhital et al. (2009, in preparation) have constructed a Galactic model, constrained with empirical stellar density profiles (Jurić et al. 2008; Bochanski et al. 2009) and disk velocity distributions (Bochanski et al. 2007), to assess the physical association of wide binary systems. The Monte Carlo model recreates a random distribution of stars in an $1800'' \times 1800''$ region of sky, centered on the coordinates of a given binary system, and out to a heliocentric distance of 2500 pc. As all the simulated stars are non-associated, the number of stars found within the separation of the binary is a measure of the number of chance alignments expected at that position in the Galaxy. In 10^7 realizations, we found the probability of chance alignment on the sky to be 0.27%. Importantly, none of the projected matches were within the range of spectrophotometric distances estimated for the 2MASS J1550+1455 components, corresponding to a $\lesssim 10^{-7}$ probability of positional coincidence.

Based on these various lines of evidence, we conclude that 2MASS J1550+1455 is a physically bound L dwarf binary.

4. DISCUSSION

For an estimated distance of 33 ± 3 pc, we infer a projected separation of 30 ± 3 AU for the components of

2MASS J1550+1455, making it the widest L dwarf-L dwarf pair identified to date. It is $\sim 20\%$ wider in physical separation than the L1.5+L4.5 pair 2MASS J1520022-442242AB ($a = 22\pm 2$ AU; Burgasser et al. 2007; Kendall et al. 2007), although that system has a wider angular separation ($1''.174\pm 0''.016$). Based on its separation and estimated component masses (Table 3), we estimate a minimum orbital period $P \gtrsim 400$ –500 yr.

The extremity of its separation does not necessarily make 2MASS J1550+1455 an unusually wide VLM pair. Burgasser et al. (2003b) quantified an empirical relation between the maximum separation limit for VLM pairs in the field and their total mass: a_{max} (AU) = 1400 $(M_{\text{tot}}/M_{\odot})^2$, applicable for systems with $M_{\text{tot}} \lesssim 0.2 M_{\odot}$. The projected separation of 2MASS J1550+1455 is within a factor of two of this limit, $a_{\text{max}} = 16$ –35 AU for ages of 0.5–5 Gyr based on the estimated masses listed in Table 3. The projected binding energy of this system, $-U_g \equiv GM_1M_2/a \approx (2\text{--}4)\times 10^{42}$ erg, is also near empirical limits encompassing the majority of VLM field systems (Close et al. 2003, 2007). In contrast, a handful of slightly more massive late-type M dwarf/L dwarf VLM pairs have been identified in the field that break these empirical limits, with separations exceeding 1000 AU (Caballero 2007b; Artigau et al. 2007; Radigan et al. 2009); there have also been found comparably wide, weakly bound low-mass brown dwarf pairs in nearby young star forming regions and associations (e.g., Luhman 2004; Caballero et al. 2006; Jayawardhana & Ivanov 2006; Close et al. 2007; Béjar et al. 2008; however, see Kraus & Hillenbrand 2009). In the context of these systems, it is clear that 2MASS J1550+1455 is in no sense an unusually wide system.

What makes 2MASS J1550+1455 potentially interesting is the fact that both components have estimated masses near the lithium burning minimum mass limit, $\sim 0.06 M_{\odot}$ for solar metallicity (Chabrier & Baraffe 1997; Burrows et al. 2001). This makes it a potential target for applying the binary lithium age-dating technique first proposed by Liu & Leggett (2005) for VLM pairs. Specifically, if the 6708 Å Li I absorption line is present in the spectrum of the secondary of a coeval VLM pair (indicating a mass $\lesssim 0.06 M_{\odot}$ and a lower age bound) but not the primary (indicating a mass $\gtrsim 0.06 M_{\odot}$ and an upper age bound), one obtains a finite constraint on the system age.⁸ The absence of the Li I line in the combined-light optical spectrum (Figure 2) is in fact promising, as it indicates that lithium is depleted in the atmosphere of the primary. This places an age constraint of $\tau \gtrsim 0.55$ Gyr based on the estimated T_{eff} of this component (including uncertainty) and the evolutionary models of Burrows et al. (1997). The lack of a clear Li I line may also indicate that lithium is depleted in the secondary as well; alternately, the line may be obscured by the relatively bright continuum from the primary. Using as a template spectral data for the L3 spectral standard 2MASS J1146345+223053, a source which ex-

⁷ We included small corrections to the relative magnitudes in converting from MKO to 2MASS photometric systems: 0.009, -0.006 and -0.003 mag in the J -, H - and K/K_s -bands respectively, calculated directly from the spectral data. See also Stephens & Leggett (2004).

⁸ This age-dating technique parallels the lithium depletion boundary technique used to date 10–200 Myr-old clusters (e.g., Magazzú et al. 1993; Bildsten et al. 1997; Stauffer et al. 1998), but is applicable for older field systems straddling the lithium burning minimum mass.

hibits Li I absorption (Kirkpatrick et al. 1999, Figure 2), and assuming a ~ 1 mag brightness difference in the 6708 Å region, we determined that a signal-to-noise ratio of 20 or better is required to detect Li I absorption from the secondary alone. In contrast, SDSS data for 2MASS J1550+1455 have a signal-to-noise of roughly 5 in this region. Hence, we cannot rule out the presence of the Li I line in the secondary. If this line is present, it would indicate a bounded age constraint of $0.55 \lesssim \tau \lesssim 0.8$ Gyr for the system (the corresponding constraint based on the Baraffe et al. 2003 evolutionary models are $0.6 \lesssim \tau \lesssim 1.1$ Gyr).

Such a young age is not inconsistent with the kinematics of 2MASS J1550+1455. The inferred space velocities, $[U, V, W] = [26 \pm 6, 0 \pm 4, -14 \pm 7]$ km s⁻¹ evaluated in the local standard of rest (Dehnen & Binney 1998), are nominally consistent with that of a young, thin disk system. The $J - K_s$ colors of the primary is slightly blue for its inferred type, since $\langle J - K_s \rangle \approx 1.6 - 1.7$ mag for L3 dwarfs (Kirkpatrick et al. 2000; Faherty et al. 2009). This could be an indication of an older age, since unusually blue near-infrared colors for VLM dwarfs have been associated with both older kinematics and higher surface gravities (e.g., Knapp et al. 2004; Faherty et al. 2009). However, variations in cloud properties can also produce variations in near-infrared color, an effect most pronounced in mid-type L dwarfs (Chiu et al. 2006; Burgasser et al. 2008b). Resolved optical spectroscopy would settle this issue, and could identify 2MASS J1550+1455 as an important age standard for VLM studies.

5. SUMMARY

We have resolved the L dwarf 2MASS J1550+1455 into a 0.9 visual binary with L3.5 and L4 components. Evidence based on the common proper motion, common spectrophotometric distance and low probability of random alignment confirms this system as a physically bound pair. While 2MASS J1550+1455 has the widest projected physical separation of any L dwarf-L dwarf binary identified to date, 30 ± 3 AU at an estimated distance of 33 ± 3 pc, it is not unusual for VLM multiples in the field. The effective temperatures of its components and lack of Li I absorption in its combined light spectrum identify 2MASS J1550+1455 as a good can-

didate for determining a precise systemic age through the binary lithium age-dating technique of Liu & Leggett (2005), necessitating resolved optical spectroscopy that is eminently feasible for this well-separated pair.

The authors would like to thank telescope operator Paul Sears and instrument specialists John Rayner for their assistance during the IRTF observations, I. N. Reid and K. L. Cruz for their helpful input in the preparation of the manuscript, and J. A. Caballero for his thorough and expert review. This publication makes use of data from the Two Micron All Sky Survey, which is a joint project of the University of Massachusetts and the Infrared Processing and Analysis Center, and funded by the National Aeronautics and Space Administration and the National Science Foundation. 2MASS data were obtained from the NASA/IPAC Infrared Science Archive, which is operated by the Jet Propulsion Laboratory, California Institute of Technology, under contract with the National Aeronautics and Space Administration. Funding for the SDSS and SDSS-II has been provided by the Alfred P. Sloan Foundation, the Participating Institutions, the National Science Foundation, the U.S. Department of Energy, the National Aeronautics and Space Administration, the Japanese Monbukagakusho, the Max Planck Society, and the Higher Education Funding Council for England. The SDSS is managed by the Astrophysical Research Consortium for the participating institutions (<http://www.sdss.org>). This research has made use of the SIMBAD database, operated at CDS, Strasbourg, France; the Very-Low-Mass Binaries Archive housed at <http://www.vlmbinaries.org> and maintained by Nick Siegler, Chris Gelino, and Adam Burgasser; and the M, L, and T dwarf compendium housed at DwarfArchives.org and maintained by Chris Gelino, Davy Kirkpatrick, and Adam Burgasser. The authors wish to recognize and acknowledge the very significant cultural role and reverence that the summit of Mauna Kea has always had within the indigenous Hawaiian community. We are most fortunate to have the opportunity to conduct observations from this mountain.

Facilities: IRTF (SpeX)

REFERENCES

- Abazajian, K. N., et al. 2009, *ApJS*, 182, 543
 Allen, P. R. 2007, *ApJ*, 668, 492
 Allers, K. N., et al. 2007, *ApJ*, 657, 511
 Artigau, É., Lafrenière, D., Doyon, R., Albert, L., Nadeau, D., & Robert, J. 2007, *ApJ*, 659, L49
 Baraffe, I., Chabrier, G., Barman, T. S., Allard, F., & Hauschildt, P. H. 2003, *A&A*, 402, 701
 Basri, G., & Reiners, A. 2006, *AJ*, 132, 663
 Bate, M. R., Bonnell, I. A., & Bromm, V. 2002, *MNRAS*, 332, L65
 Béjar, V. J. S., Zapatero Osorio, M. R., Pérez-Garrido, A., Álvarez, C., Martín, E. L., Rebolo, R., Villó-Pérez, I., & Díaz-Sánchez, A. 2008, *ApJ*, 673, L185
 Bildsten, L., Brown, E. F., Matzner, C. D., & Ushomirsky, G. 1997, *ApJ*, 482, 442
 Bochanski, J. J., Hawley, S. L., Covey, K. L., Reid, I. N., West, A. A., Golimowski, D. A., & Ivezić, Ž. 2009, *AJ*
 Bochanski, J. J., Munn, J. A., Hawley, S. L., West, A. A., Covey, K. R., & Schneider, D. P. 2007, *AJ*, 134, 2418
 Boss, A. P. 2001, *ApJ*, 551, L167
 Burgasser, A. J. 2007, *ApJ*, 659, 655
 Burgasser, A. J., Geballe, T. R., Leggett, S. K., Kirkpatrick, J. D., & Golimowski, D. A. 2006, *ApJ*, 637, 1067
 Burgasser, A. J., Kirkpatrick, J. D., Burrows, A., Liebert, J., Reid, I. N., Gizis, J. E., McGovern, M. R., Prato, L., & McLean, I. S. 2003a, *ApJ*, 592, 1186
 Burgasser, A. J., Kirkpatrick, J. D., Reid, I. N., Brown, M. E., Miskey, C. L., & Gizis, J. E. 2003b, *ApJ*, 586, 512
 Burgasser, A. J., Liu, M. C., Ireland, M. J., Cruz, K. L., & Dupuy, T. J. 2008a, *ApJ*, 681, 579
 Burgasser, A. J.,Looper, D. L., Kirkpatrick, J. D., Cruz, K. L., & Swift, B. J. 2008b, *ApJ*, 674, 451
 Burgasser, A. J.,Looper, D. L., Kirkpatrick, J. D., & Liu, M. C. 2007, *ApJ*, 658, 557
 Burgasser, A. J., & McElwain, M. W. 2006, *AJ*, 131, 1007
 Burrows, A., Hubbard, W. B., Lunine, J. I., & Liebert, J. 2001, *Reviews of Modern Physics*, 73, 719
 Burrows, A., Marley, M., Hubbard, W. B., Lunine, J. I., Guillot, T., Saumon, D., Freedman, R., Sudarsky, D., & Sharp, C. 1997, *ApJ*, 491, 856
 Caballero, J. A. 2007a, *ApJ*, 667, 520

- . 2007b, *A&A*, 462, L61
- Caballero, J. A., Martín, E. L., Dobbie, P. D., & Barrado Y Navascués, D. 2006, *A&A*, 460, 635
- Chabrier, G., & Baraffe, I. 1997, *A&A*, 327, 1039
- . 2000, *ARA&A*, 38, 337
- Chabrier, G., Baraffe, I., Leconte, J., Gallardo, J., & Barman, T. 2009, in *American Institute of Physics Conference Series*, Vol. 1094, American Institute of Physics Conference Series, ed. E. Stempels, 102–111
- Chiu, K., Fan, X., Leggett, S. K., Golimowski, D. A., Zheng, W., Geballe, T. R., Schneider, D. P., & Brinkmann, J. 2006, *AJ*, 131, 2722
- Close, L. M., Siegler, N., Freed, M., & Biller, B. 2003, *ApJ*, 587, 407
- Close, L. M., et al. 2007, *ApJ*, 660, 1492
- Cruz, K. L., Reid, I. N., Liebert, J., Kirkpatrick, J. D., & Lowrance, P. J. 2003, *AJ*, 126, 2421
- Cruz, K. L., et al. 2007, *AJ*, 133, 439
- Cushing, M. C., Vacca, W. D., & Rayner, J. T. 2004, *PASP*, 116, 362
- Dehnen, W., & Binney, J. J. 1998, *MNRAS*, 298, 387
- Dupuy, T. J., Liu, M. C., & Ireland, M. J. 2009, *ApJ*, 692, 729
- Faherty, J. K., Burgasser, A. J., Cruz, K. L., Shara, M. M., Walter, F. M., & Gelino, C. R. 2009, *AJ*, 137, 1
- Geballe, T. R., et al. 2002, *ApJ*, 564, 466
- Henry, T. J., Jao, W.-C., Subasavage, J. P., Beaulieu, T. D., Ianna, P. A., Costa, E., & Méndez, R. A. 2006, *AJ*, 132, 2360
- Jameson, R. F., Casewell, S. L., Bannister, N. P., Lodieu, N., Keresztes, K., Dobbie, P. D., & Hodgkin, S. T. 2008, *MNRAS*, 384, 1399
- Jayawardhana, R., & Ivanov, V. D. 2006, *Science*, 313, 1279
- Jiang, I.-G., Laughlin, G., & Lin, D. N. C. 2004, *AJ*, 127, 455
- Joergens, V., & Müller, A. 2007, *ApJ*, 666, L113
- Jurić, M., et al. 2008, *ApJ*, 673, 864
- Kasper, M., Burrows, A., & Brandner, W. 2009, *ApJ*, 695, 788
- Kendall, T. R., Jones, H. R. A., Pinfield, D. J., Pokorný, R. S., Folkes, S., Weights, D., Jenkins, J. S., & Mauron, N. 2007, *MNRAS*, 374, 445
- Kirkpatrick, J. D. 2005, *ARA&A*, 43, 195
- Kirkpatrick, J. D., Reid, I. N., Liebert, J., Gizis, J. E., Burgasser, A. J., Monet, D. G., Dahn, C. C., Nelson, B., & Williams, R. J. 2000, *AJ*, 120, 447
- Kirkpatrick, J. D., et al. 1999, *ApJ*, 519, 802
- Knapp, G. R., et al. 2004, *AJ*, 127, 3553
- Kraus, A. L., & Hillenbrand, L. A. 2009, *ArXiv e-prints*
- Liu, M. C., & Leggett, S. K. 2005, *ApJ*, 634, 616
- Looper, D. L., Gelino, C. R., Burgasser, A. J., & Kirkpatrick, J. D. 2008a, *ApJ*, 685, 1183
- Looper, D. L., et al. 2008b, *ApJ*, 686, 528
- Luhman, K. L. 2004, *ApJ*, 614, 398
- Magazzú, A., Martín, E. L., & Rebolo, R. 1993, *ApJ*, 404, L17
- Martín, E. L., Brandner, W., Bouy, H., Basri, G., Davis, J., Deshpande, R., & Montgomery, M. M. 2006, *A&A*, 456, 253
- McElwain, M. W., & Burgasser, A. J. 2006, *AJ*, 132, 2074
- McLean, I. S., McGovern, M. R., Burgasser, A. J., Kirkpatrick, J. D., Prato, L., & Kim, S. S. 2003, *ApJ*, 596, 561
- Phan-Bao, N., Forveille, T., Martín, E. L., & Delfosse, X. 2006, *ApJ*, 645, L153
- Pier, J. R., Munn, J. A., Hindsley, R. B., Hennessy, G. S., Kent, S. M., Lupton, R. H., & Ivezić, Z. 2003, *AJ*, 125, 1559
- Radigan, J., Lafrenière, D., Jayawardhana, R., & Doyon, R. 2009, *ApJ*, 698, 405
- Rayner, J. T., Toomey, D. W., Onaka, P. M., Denault, A. J., Stahlberger, W. E., Vacca, W. D., Cushing, M. C., & Wang, S. 2003, *PASP*, 115, 362
- Reid, I. N., Burgasser, A. J., Cruz, K. L., Kirkpatrick, J. D., & Gizis, J. E. 2001, *AJ*, 121, 1710
- Reid, I. N., Hawley, S. L., & Gizis, J. E. 1995, *AJ*, 110, 1838
- Reid, I. N., Kirkpatrick, J. D., Liebert, J., Gizis, J. E., Dahn, C. C., & Monet, D. G. 2002, *AJ*, 124, 519
- Reipurth, B., & Clarke, C. 2001, *AJ*, 122, 432
- Simons, D. A., & Tokunaga, A. 2002, *PASP*, 114, 169
- Skrutskie, M. F., et al. 2006, *AJ*, 131, 1163
- Stassun, K. G., Mathieu, R. D., & Valenti, J. A. 2006, *Nature*, 440, 311
- Stauffer, J. R., Schultz, G., & Kirkpatrick, J. D. 1998, *ApJ*, 499, L199+
- Stephens, D. C., & Leggett, S. K. 2004, *PASP*, 116, 9
- Tokunaga, A. T., & Kobayashi, N. 1999, *AJ*, 117, 1010
- Tokunaga, A. T., Simons, D. A., & Vacca, W. D. 2002, *PASP*, 114, 180
- Vacca, W. D., Cushing, M. C., & Rayner, J. T. 2003, *PASP*, 115, 389
- York, D. G., et al. 2000, *AJ*, 120, 1579
- Zapatero Osorio, M. R., Lane, B. F., Pavlenko, Y., Martín, E. L., Britton, M., & Kulkarni, S. R. 2004, *ApJ*, 615, 958

TABLE 3
 PROPERTIES OF 2MASS J15500845+1455180AB

Parameter	2MASS J1550+1455A	2MASS J1550+1455B
Near Infrared Spectral Type	L3.5	L4
i (mag)	19.75±0.09	20.56±0.19
z (mag)	17.95±0.09	18.68±0.17
J (mag)	15.34±0.04	15.76±0.05
H (mag)	14.42±0.05	14.70±0.05
K_s (mag)	13.91±0.04	14.13±0.04
$i - z$ (mag)	1.80±0.13	1.88±0.25
$J - K_s$ (mag)	1.43±0.06	1.63±0.06
$T_{\text{eff}}^{\text{a}}$ (K)	1910±110	1840±110
Mass at 0.5 Gyr ^b (M_{\odot})	0.056	0.054
Mass at 1 Gyr ^b (M_{\odot})	0.070	0.067
Mass at 5 Gyr ^b (M_{\odot})	0.079	0.078
Distance ^c (pc)	31±3	34±3
	2MASS J1550+1455AB	
Optical Spectral Type	L3	
Distance (pc)	33±3	
Projected Separation (AU)	30±3	
V_{tan} (km s ⁻¹)	26±3	
V_{rad} (km s ⁻¹)	-7±12	
U, V, W (km s ⁻¹)	26±6, 0±4, -14±7	

^a Estimate based on the T_{eff} /spectral type relation ofLooper et al. (2008a) and including uncertainties in relation and component classifications (± 0.3 - 0.4 subtypes).

^b Estimates based on the evolutionary models of Burrows et al. (1997).

^c Estimate based on the M_J /spectral type relation of Cruz et al. (2003); uncertainties include photometric uncertainties and scatter in the Cruz et al. relation.